Brake, A. J., Merryweather, J. P., Coit, D., Heberlein, U. A., Masiarz, F. R., Mullenbach, G. T., Urdea, M. S., Valenzuela, P., & Barr, P. J. (1984) *Proc. Natl. Acad. Sci. U.S.A. 81*, 4642-4646.
Burgess, A. W., Knesel, J., Sparrow, L. G., Nicola, N. A., & Nice, E. C. (1982) *Proc. Natl. Acad. Sci. U.S.A. 79*, 5753-5757.
Carpenter, G. (1980) *Science (Washington, D.C.) 210*, 198-199.
Carpenter, G. (1985) *J. Cell Sci., Suppl. 3*, 1-9.
Carpenter, G., & Cohen, S. (1979) *Annu. Rev. Biochem. 48*, 193-216.
Cohen, S. (1962) *J. Biol. Chem. 237*, 1555-1562.
Cohen, S., & Carpenter, G. (1975) *Proc. Natl. Acad. Sci. U.S.A. 72*, 1317-1321.
DiAugustine, R. P., Walker, M. P., Klapper, D. G., Grove, R. I., Willis, W. D., Harvano, D. J., & Hernandez, O. (1985) *J. Biol. Chem. 260*, 2807-2811.
Gregory, H. (1975) *Nature (London) 257*, 325-327.
Gregory, H., & Preston, B. M. (1977) *Int. J. Pept. Protein Res. 9*, 107-118.
Heath, W. F., & Merrifield, R. B. (1986) *Proc. Natl. Acad. Sci. U.S.A. 83*, 6367-6371.
Hirata, Y., & Orth, D. N. (1979) *J. Clin. Endocrinol. Metab. 49*, 481-483.
Hollenberg, M. P., & Gregory, H. (1980) *Mol. Pharmacol. 17*, 314-320.
Julius, D., Blair, L., Brake, A., Sprague, G., & Thorner, J. (1983) *Cell (Cambridge, Mass.) 32*, 839-852.
Julius, D., Brake, A., Blair, L., Kemisawa, R., & Thorner, J. (1984) *Cell (Cambridge, Mass.) 37*, 1075-1089.
Oka, Y., & Orth, D. N. (1983) *J. Clin. Invest. 72*, 249-259.
Oka, T., Sakamoto, S., Miyoshi, K. I., Fuwa, T., Yoda, K., Yamasaki, M., Tamura, G., & Miyake, T. (1985) *Proc. Natl. Acad. Sci. U.S.A. 82*, 7212-7216.
Petrides, P. E., Böhlen, P., & Shively, J. E. (1984) *Biochem. Biophys. Res. Commun. 125*, 218-228.
Petrides, P. E., Hosang, M., Shooter, E., Esch, F. S., & Böhlen, P. (1985) *FEBS Lett. 187*, 89-95.
Rozengurt, E., & Heppel, L. A. (1975) *Proc. Natl. Acad. Sci. U.S.A. 72*, 4492-4495.
Savage, C. R., & Harper, R. (1981) *Anal. Biochem. 111*, 195-202.
Savage, C. R., Hash, J. H., & Cohen, S. (1973) *J. Biol. Chem. 248*, 7669-7672.
Shechter, Y. (1986) *J. Biol. Chem. 261*, 66-70.
Simpson, R. J., Smith, J. A., Moritz, R. L., O'Hare, M. J., Rudland, P. S., Morrison, J. R., Lloyd, Ch. J., Grego, B., Burgess, A. W., & Nice, E. C. (1985) *Eur. J. Biochem. 153*, 629-637.
Smith, J., Cook, E., Fotheringham, I., Pheby, S., Derbyshire, R., Eaton, M. A. W., Doel, M., Lilly, D. M., Pardon, J. F., Patel, T., Lewis, M., & Bell, L. D. (1982) *Nucleic Acids Res. 10*, 4467-4482.
Storring, P. I., & Tiplady, R. J. (1984) *Anal. Biochem. 141*, 43-54.
Stötzler, D., Kiltz, H. H., & Duntze, W. (1976) *Eur. J. Biochem. 69*, 397-400.
Urdea, M. S., Merryweather, J. P., Mullenbach, G. T., Coit, T., Herberlein, U., Valenzuela, P., & Barr, P. J. (1983) *Proc. Natl. Acad. Sci. U.S.A. 86*, 7461-7465.

Determination of Local Conformational Stability in Fragment 96-133 of Bovine Growth Hormone by High-Resolution ^{1}H NMR Spectroscopy

Paul R. Gooley,‡ Scott M. Plaisted, David N. Brems, and Neil E. MacKenzie*
Control Division, Building 259-2, The Upjohn Company, 7000 Portage Road, Kalamazoo, Michigan 49001
Received April 7, 1987; Revised Manuscript Received September 2, 1987

ABSTRACT: The specific assignment of resonances in the 400-MHz nuclear magnetic resonance (NMR) spectrum of fragment 96-133 (AII) of bovine growth hormone (bSt) is described. Assignments have been made with homonuclear two-dimensional techniques, in particular that of sequential resonance assignment. Complete assignments were possible for the spin systems of 16 residues out of a total of 38 and partial assignments for another 5. Assignment of resonances to either residue type or a class of residue was possible for a number of other spin systems. Analysis of the type of nuclear Overhauser effect (NOE) indicates that segments 96-110 and 130-133 are nonregular stable structures and that the segment 111-127, which putatively spans the α-helix, is not sufficiently stable to generate NOEs.

Pituitary bovine growth hormone (bSt) is a globular protein consisting of 191 amino acids. Partial tryptic digestion of bSt yields a fragment, AII (residues 96-133), which retains measurable biological activity (Sonenberg et al., 1968; Yamasaki et al., 1975). The primary sequence of the peptide AII is shown in Figure 1. On the basis of the primary sequence of intact bSt, Chou-Fasman predictions (Chou & Fasman, 1974a,b) find a helical region in the segment 111-127 and β-sheet structure in the pentapeptide 101-105. AII encompasses both these regions, and indeed, circular dichroism studies show that at pH 4 AII is composed of 32% helix and 10% β-sheet, which decreases to 7% helix and 6% β-sheet at pH 9 (Chen & Sonenberg, 1977). The helical content of AII has also been found to be concentration, pH, and ionic strength dependent (Brems et al., unpublished results).

Fragments derived from helical regions of intact protein are generally devoid of any ordered structure leading to the conclusion that tertiary interactions are necessary to stabilize the

* Address correspondence to this author.
‡ Present address: Department of Molecular Biophysics and Biochemistry, School of Medicine, Yale University, New Haven, CT 06510.

0006-2960/88/0427-0802$01.50/0

```
 96                 100                 105
Val-Phe-Thr-Asn-Ser-Leu-Val-Phe-Gly-Thr-

                   110                 115
Ser-Asp-Arg-Val-Tyr-Glu-Lys-Leu-Lys-Asp-

                   120                 125
Leu-Glu-Glu-Gly-Ile-Leu-Ala-Leu-Met-Arg-

                   130         133
Glu-Leu-Glu-Asp-Gly-Thr-Pro-Arg
```

FIGURE 1: Amino acid sequence of fragment 96–133 (AII) of bSt (Graf & Li, 1974).

helix. A reported exception is the S peptide helix from ribonuclease S (Brown & Klee, 1971; Kim & Baldwin, 1984; Shoemaker et al., 1985). Low temperatures, however, are necessary to promote helix formation, and a ^{1}H NMR study at room temperature indicated that the S peptide did not show a preferred conformation exhibiting ordered structure (Rico et al., 1983; Gallego et al., 1983). An interesting study showed a number of amide protons of S peptide had significantly reduced exchange rates when the S peptide was bound to the S protein, indicating that interactions between residues of the S peptide and the S protein stabilized the S peptide conformation (Kuwajima & Baldwin, 1983).

Although linear peptide fragments have not shown stable helix, a stable reverse turn in a nonapeptide from hemagglutin has been observed (Dyson et al., 1985) suggesting that this structural facet may not require interactions between other parts of the protein to maintain stability. Recently, the Ω-loop, a type of nonregular structure common in many proteins, has been characterized as a compact stable substructure which may fold independently of the parent protein (Leszczynski & Rose, 1986). These loops are generally found on the surface of proteins where they may play essential roles in molecular recognition and biological activity.

There are no reports specifying the details of the helix of AII observed by circular dichroism, and for this reason we initiated a ^{1}H NMR study at 400 MHz of AII in solution. In the course of our study we have observed a stable Ω-loop spanning residues 100–110. Here we present the assignments of the proton resonances of the residues in the peptide segments 96–110 and 130–133.

Materials and Methods

The fragment 96–133 (AII) was obtained by partial tryptic digestion and isolated as described by Graf and Li (1974). The purity of AII was determined by the criteria of a single component by high-performance liquid chromatography (HPLC) reverse-phase chromatography (Brems et al., 1985) and polyacrylamide electrophoresis (Swank & Munkres, 1971).

Peptide samples were prepared by dissolving fresh peptide in either ^2H_2O or H_2O and adjusting the pH with small amounts of dilute deuteriated or nondeuteriated HCl and NaOH as required. Reported pH values are pH meter readings uncorrected for isotope effects. To minimize accumulation of salt and paramagnetic metal ions, peptide samples were regularly freeze-dried and chromatographed in distilled water on Sephadex G-10 columns.

^{1}H NMR spectra were recorded at 400 MHz on a Bruker AM-400 or a Varian XL-400 spectrometer; 5-mm outer diameter spinning sample tubes (Wilmad Glass Co., 528-PP or 507-PP grade) were used. Typical one-dimensional spectral acquisition parameters were as follows: spectral width 4000 Hz, 90° radio-frequency pulse, 1.0-s delay between transients,

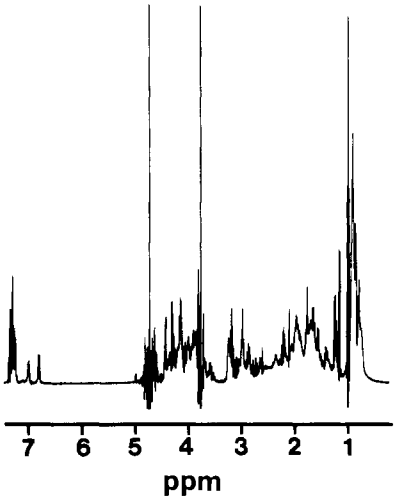

FIGURE 2: The 400-MHz ^{1}H NMR spectrum of 2 mM AII in ^2H_2O, pH 3.1 at 25 °C. Spectral parameters are described under Materials and Methods. The resonance at 2.2 ppm is acetate, at 3.75 ppm dioxane, and at 4.7 ppm residual water.

16 384 time-domain addresses. Prior to Fourier transformation the spectra were multiplied by a Lorentz–Gauss window function and zero-filled to 32 768 addresses. Chemical shifts are expressed in ppm downfield from 4,4-dimethyl-4-silapentane-1-sulfonate but were measured from a trace of internal dioxane at 3.751 ppm.

Two dimensional double quantum filtered phase-sensitive homonuclear correlated (DQF-COSY) spectra were recorded with the pulse sequence t_0–90°–t_1–90°–Δ–90°–t_2 (Rance et al., 1983), where t_1 and t_2 are the evolution and detection periods, respectively. Two-dimensional phase-sensitive nuclear Overhauser enhancement (NOESY) spectra were recorded with the pulse sequence t_0–90°–t_1–90°–τ_m–90°–t_2 (Jeener et al., 1979), where τ_m is the mixing period, usually 200 ms. Experiments acquired on the Bruker AM-400 used the time proportional phase incrementation scheme (Redfield & Kunz, 1975; Marion & Wüthrich, 1983), and experiments acquired on the Varian XL-400 used the hypercomplex scheme (States et al., 1982). Experiments were recorded with quadrature detection in both directions; at least 256 t_1 values were acquired for DQF-COSY and NOESY spectra and with each free induction decay consisting of 2048 data addresses. For both ^2H_2O and H_2O experiments the spectral width was 4000 Hz in both dimensions. The water resonance was suppressed by low-power irradiation at all times except during acquisition. Prior to Fourier transformation the data were multiplied by a phase-shifted sine bell function in the t_1 domain and a phase-shifted sine squared bell function in the t_2 domain and zero filled to 4096 (t_2) and 1024 (t_1) data addresses.

Results

Aromatic Region. Figure 2 shows a one-dimensional spectrum of 2 mM AII in ^2H_2O at pH 3.1 and 25 °C. The aromatic region consists of a complex multiplet at 7.2 ppm and two doublets at 6.99 and 6.78 ppm. The multiplet is assigned to the ring protons of Phe-97 and -103. The doublet at 6.99 ppm (J_{ortho} = 7.3 Hz) is assigned to the H-2,6 protons and the doublet at 6.78 ppm (J_{ortho} = 7.0 Hz) to the H-3,5 protons of Tyr-110, the only Tyr in AII. The chemical shifts and coupling constants for these resonances are similar to those for Phe and Tyr in small peptides (Bundi & Wüthrich, 1979).

Short-range NOEs between the ring protons nearest the peptide backbone and the β-protons can be used to assign the H^β resonances of the aromatic residues (Billeter et al., 1982). In Figure 3B each Phe ring system of AII shows NOEs to only

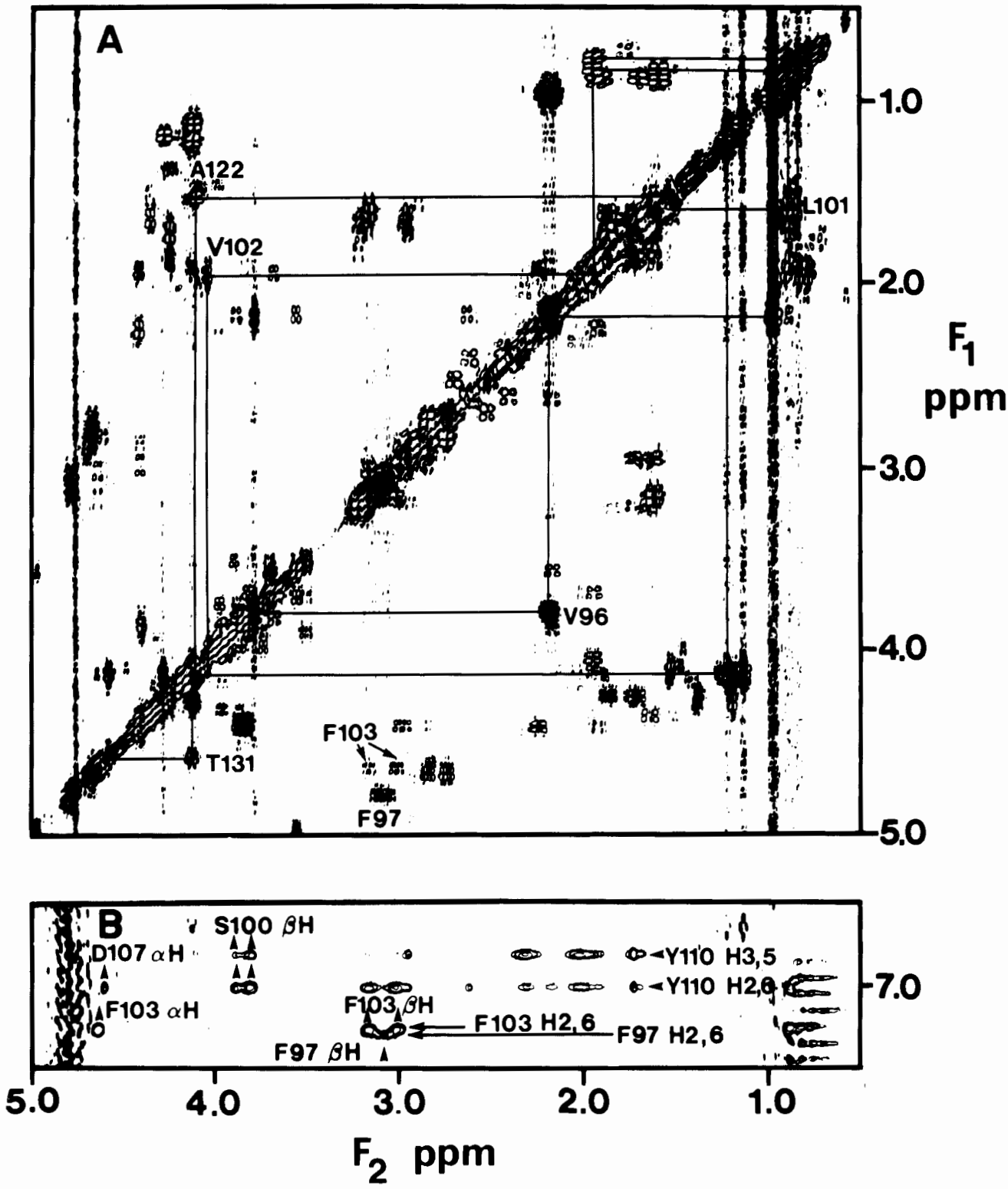

FIGURE 3: Contour plots of homonuclear 2D spectra of 8 mM AII in ^2H_2O, pH 3.1 at 25 °C. (A) The aliphatic region of a DQF-COSY spectrum showing J connectivities for the complete spin systems of Val-96, Phe-97, Val-102, Phe-103, Ala-122, and Thr-131. The H^{γ}–$H^{\delta}{}_2$ couplings of Leu-101 are also indicated. (B) The spectral region from a NOESY spectrum showing NOEs from the ring systems of Phe-97, Phe-103, and Tyr-110 to aliphatic protons. NOE connectivities are indicated from the H-2,6 of Phe-103 to its H^{α} and both H^{β} and from the H-2,6 of Phe-97 to one H^{β}. Long-range NOEs from the Tyr ring protons to the H^{β} of Ser-100 and Phe-103 and the H^{α} of Asp-107 are shown.

one AMX (H^{α}–$H^{\beta}2$) spin system. One Phe shows intense NOEs to two H^{β} and to one H^{α} proton while the other Phe shows an NOE to one H^{β} proton. No other NOEs are observed from the ring protons of the Phe residues. The H^{β} and the H^{α} resonances of the first Phe show J connectivities to each other in DQF-COSY spectra (Figure 3A). The H^{β} resonance of the second Phe shows a J connectivity to an H^{α} resonance, but no other couplings are observed from this H^{α}, suggesting that the two H^{β} protons are equivalent. In Figure 3B and H-2,6 and H-3,5 of Tyr-110 show many NOEs to various protons; however, as both sets of ring protons show NOEs to the same H^{β} protons at 3.88, 3.16, and 3.00 ppm we cannot assign these resonances to the H^{β} of Tyr-110. In fact, the resonance at 3.88 ppm is assigned to the H^{β} of Ser-100, and the resonance at 3.16 and 3.00 ppm are assigned to the H^{β} of Phe-103 (see sequential assignments below). The H-2,6

Table I: Specific Assignment (ppm) of Resonances of AII[a]

residue	NH	H^{α}	H^{β}	other	sequential NOE	residue	NH	H^{α}	H^{β}	other	sequential NOE
Val-96		3.77	2.17	H^{γ}_3 0.99	H^{α} Val-96–NH Phe-97	Ser-106	8.40	4.36	3.98, 3.88		H^{α} Ser-106–NH Asp-107
						Asp-107	8.44	4.60	2.83		
				H^{γ}_3 0.98	H^{β} Val-96–NH Phe-97	Arg-108					
						Val-109[b]	7.88	3.60	2.13	H^{γ}_3 0.84	
Phe-97	8.73	4.80	3.07	H-2,6 7.24	H^{α} Phe-97–NH Thr-98					H^{γ}_3 0.94	
						Tyr-110				H-2,6 6.99	
					H^{β} Phe-97–NH Thr-98					H-3,5 6.78	
						Glu-111					
Thr-98	8.13	4.28	4.13	H^{γ}_3 1.13	H^{α} Thr-98–NH Asn-99	Lys-112					
						Leu-113					
					H^{β} Thr-98–NH Asn-99	Lys-114					
						Asp-115					
Asn-99	8.31	4.68	2.84, 2.73	NH^{δ} 7.61	H^{α} Asn-99–NH Ser-100	Leu-116					
						Glu-117					
				NH^{δ} 6.91	H^{β} Asn-99–NH Ser-100	Glu-118					
						Gly-119		3.86, 3.73			
Ser-100	8.24	4.40	3.88, 3.81		H^{α} Ser-100–NH Leu-101	Ile-120				H^{γ} 0.93	
										H^{γ} 1.67	
Leu-101	8.21	4.35	1.62	H^{γ}_2 1.57	NH Leu-101–NH Val-102					H^{δ}_3 0.69	
						Leu-121					
				H^{δ}_3 0.81	H^{α} Leu-101–NH Val-102	Ala-122[b]	7.98	4.10	1.53		
						Leu-123					
				H^{δ}_3 0.87		Met-124				H^{ϵ}_3 1.75	
Val-102	7.86	4.03	1.93	H^{γ}_3 0.86	H^{α} Val-102–NH Phe-103	Arg-125					
						Glu-126					
				H^{γ}_3 0.80		Leu-127					
Phe-103	8.22	4.65	3.16, 3.00	H-2,6 7.22	H^{α} Phe-103–NH Gly-104	Glu-128					
						Asp-129					
					H^{β} Phe-103–NH Gly-104	Gly-130	8.07	3.97			H^{α} Gly-130–NH Thr-131
						Thr-131[c]	7.93	4.59	4.12	H^{γ}_3 1.23	H^{α} Thr-131–H^{δ} Pro-132
Gly-104	8.31	3.98			H^{α} Gly-104–NH Thr-105	Pro-132		4.36	2.24, 1.93	H^{γ}_2 1.93	H^{α} Pro-132–NH Arg-133
										H^{δ} 3.82	
Thr-105	8.06	4.25	4.30	H^{γ}_3 1.18	H^{α} Thr-105–NH Ser-106					H^{δ} 3.67	
						Arg-133	8.16	4.22	1.87, 1.71		

[a] Solution conditions were 8 mM, pH 3.1, and 25 °C. [b] Observed at 45 °C. [c] Thr-131 is split into two spin systems (see text). The second spin system is NH 8.54, H^{α} 4.64, H^{β} 4.12, and H^{γ} 1.27 ppm.

protons show an NOE to an H^{α} proton at 4.62 ppm but not to the H^{β} proton at 2.83 ppm to which it is coupled, and indeed, this spin system is sequentially assigned to Asp-107. These long-range NOEs will be discussed below.

Methyl Region. AII contains 24 methyl groups from Val-96, -102, and -109, Thr-98, -105, and -131, Leu-101, -113, -116, -121, -123, and -127, Ile-120, Ala-122, and Met-124. In Figure 2 the H^{ϵ}_3 of Met-124 resonates as a singlet at 1.75 ppm, 0.4 ppm upfield of its random coil position, and the Thr and Ala resonances occur between 1.2 and 1.6 ppm while the remaining 19 methyls resonate between 0.6 and 1.0 ppm.

The H^{α}, H^{β}, and H^{γ}_3 couplings of two Thr can be easily assigned in DQF-COSY spectra (Figure 3A). Only the H^{γ}_3 to H^{β} of the third Thr is observed, suggesting that the H^{α} and H^{β} chemical shifts are coincident, but as this coupling and the H^{α} to H^{β}_3 coupling of Ala-122 are identical in appearance in these DQF-COSY spectra, we cannot unambiguously assign the two systems (Neuhaus et al., 1985). However, the doublet at 1.53 ppm has a coupling constant of 7.5 Hz whereas the doublet at 1.18 ppm has a coupling constant of 5.5 Hz. The first doublet is close to the chemical shift and $J_{\alpha\beta}$ of the methyl of Ala residues in small peptides, viz., 1.4 ppm and 7.0 Hz, whereas the second doublet is nearer the chemical shift and $J_{\beta\gamma}$ of the methyl of Thr residues in small peptides, viz., 1.2 ppm and 6.3 Hz (Bundi & Wüthrich, 1979). In addition to the three Thr systems, a fourth spin system with resonances at 4.65, 4.12, and 1.28 ppm can be observed. These chemical shifts are very similar to those of the Thr with resonances at 4.59, 4.12, and 1.23 ppm (respectively H^{α}, H^{β}, and H^{γ}_3). This latter Thr is assigned by sequential assignments to Thr-131 (see below), and we believe the additional Thr system is due to the presence of both *cis*- and *trans*-Pro-132.

The assignment of the H^{α}, H^{β}, and $(H^{\gamma}_3)_2$ of two Val systems is readily achieved in DQF-COSY spectra at 25 °C (Figure 3A) while the third Val system could only be observed at higher temperatures (45 °C). The connectivities between the two H^{δ}_3 methyls and the γH of one Leu is clearly established in DQF-COSY spectra (Figure 3A). Linking this system to the H^{β} resonances is generally not possible in COSY spectra because the H^{γ} and H^{β} resonances overlap. However, the H^{β}–H^{β}_2 group can be connected to the H^{γ}–$(H^{\delta}_3)_2$ by NOEs between an H^{α} at 4.35 ppm and both H^{δ}_3. As the remaining 12 methyl resonances overlap, only partial assignments of two other Leu residues are possible (see Table II), although one of these assignments may be the H^{γ}_3 of Ile-120. The H^{δ}_3 of Ile-120 resonates at 0.69 ppm and shows connectivities to the two γH resonances at 0.93 and 1.67 ppm.

Other Residues. Only one of the three Gly residues in AII has sufficiently resolved H^{α} resonances at 3.73 and 3.86 ppm. The H^{α} resonances of each of the other two Gly spin systems have almost coincident chemical shifts, but these systems are assigned by the technique of sequential assignment (see below).

Excluding aromatic residues, there are six AMX spin systems, three Asp, two Ser, and one Asn, remaining to be assigned. Eight spin systems have been resolved that can be assigned to these residues. The additional spin systems lend credence to the possibility that Pro-132 exists in both cis and trans forms, and this is being further examined by ^{13}C NMR spectroscopy (Deslauriers et al., 1972).

The remaining spin systems of Glu, Met, Arg, and Lys are difficult to assign due to resonance complexity and their characteristic weak cross-peaks. However, partial assignment of several of these systems is possible, and the data are included in Table II. Three H^{γ}_2 connectivities are assigned to Glu

residues as these resonances show pH dependence in DQF-COSY spectra recorded at pH 2.6, 3.1, and 3.6 in H_2O. Due to resonance broadening the pH dependence of only one of these resonances could be followed in 1D spectra and was characterized by a pK_a value of 4.22 ± 0.20, typical of Glu residues (Keim et al., 1973; Bundi & Wüthrich, 1979). One set of these H^{γ}_2 resonances, assigned to the Glu residues, may belong to Met-124 and could be sensing the titration of a nearby carboxylate, but as the H^{ϵ}_3 of Met-124 shows little pH dependence below pH 4 the assignments are consistent with Glu. A fourth H^{γ}_2 multiplet is only observed in the DQF-COSY recorded at pH 3.1 in ^2H_2O, and hence, its pH dependence could not be derived. A likely assignment of this multiplet is either a fourth Glu or Met-124. The H^{α} resonance at 4.22 ppm, coupled to H^{β} resonances at 1.87 and 1.71 ppm, shows a pH dependence different to that of the above three H^{γ}_2 multiplets titrating with a lower pK_a. This spin system is therefore assigned to Arg-133, the C-terminus of AII.

Sequential Assignments. The above sections describe the assignments of the complete spin systems of several residues. The connection of these residues with their neighbors by the technique of sequential resonance assignment would specifically assign the spin systems (Wagner et al., 1981; Billeter et al., 1982; Wüthrich, 1986). In essence, DQF-COSY and NOESY are acquired on samples of protein dissolved in H_2O (with 10% ^2H_2O for locking). *J* connectivities are established between the H^{α} and NH spins of individual systems, and then neighboring residues are connected via short-range NOEs. In Figure 4A, NOEs are observed between the NH proton of the $i + 1$ residue and the H^{α} of the preceding i residue for the segment encompassing residues 98–104. In Figure 4B, an NOE is seen between the NH protons of Leu-101 and Val-102. Not shown in the figure are a number of NOEs between the NH of the $i + 1$ residue and the H^{β} of the preceding i residue, for example, between Phe-97 and Val-96, Thr-98 and Phe-97, Asn-99 and Thr-98, Ser-100, and Asn-99, and Gly-104 and Phe-103.

Combined DQF-COSY and NOESY spectra of AII recorded at 45 °C extend the above assignments. In Figure 5, NOEs connect the H^{α}_i and NH_{i+1} protons of neighboring residues for the segments 96–98 and 104–107. The H^{α} protons of Phe-97 and Asp-107 resonate near the water signal and therefore at 25 °C are bleached from the spectrum during water suppression. At 45 °C, however, these resonances are resolved from the water signal. The majority of the sequential NOEs observed at 25 °C are also present at 45 °C.

In NOESY spectra recorded on samples of AII in ^2H_2O, the H^{α} proton at 4.59 ppm, assigned to a Thr, shows NOEs to protons at 3.82 and 3.67 ppm. This NOE pattern would be expected between the H^{α} of Thr-131 and the H^{δ}_2 of Pro-132, where Pro-132 is in the trans conformer (Arseniev et al., 1984). In Figure 4A, the NH of Thr-131 shows a strong NOE to an H^{α} which is assigned to Gly-130. The NH of the spin system assigned to Arg-133 is connected by an NOE to the H^{α} of Pro-132. By default, the specific assignments of Val-96 and -102 and Gly-104 and -130 allow the assignments of Val-109 and Gly-119.

Table I summarizes the chemical shifts of all the assigned spin systems along with the sequential NOEs. Included in this table are several specific assignments of residues that are unique to the primary sequence of AII. Table II contains a number of partial spin systems that cannot be connected by sequential NOEs and therefore are not specifically assigned. These spin systems, however, can be categorized as residue type or into a class of residue.

Table II: Nonspecific Assignment (ppm) of Resonances of AII[a]

type of residue[b]	NH	H^{α}	H^{β}	other
AMX 1[c]		4.41	2.98, 2.85	
AMX 2	8.14	4.71	2.93	
AMX 3[d]	8.08	4.80	3.22, 2.84	
AMX 4[d]		3.88	3.70, 3.50	
AMX 5		4.95	3.71, 3.56	
long chain 1	8.10	4.17	1.96	
long chain 2[d,e]		4.13	1.85, 1.53	
long chain 3		4.41	2.30, 1.97	
long chain 4[d,e]	7.52	4.17	2.17	
long chain 5[d]	8.14	4.31		
long chain 6[d]	8.25	4.28		
long chain 7	7.82	4.15	2.26	
Glu[f]				H^{γ}_2 2.52, 2.70
				H^{γ}_2 2.40, 2.61
				H^{γ}_2 2.16, 2.62
Met-124 or Glu[g]				H^{γ}_2 2.45, 2.36
Arg 1[c]				NH^{ϵ} 7.15, H^{δ}_2 3.15, H^{γ}_2 1.61
Arg 2				NH^{ϵ} 7.31, H^{δ}_2 3.19, H^{γ}_2 1.65
Arg 3				NH^{ϵ} 7.23, H^{δ}_2 3.17
Arg 4				NH^{ϵ} 7.25, H^{δ}_2 3.21
Lys 1				H^{ϵ}_2 2.94, H^{δ}_2 1.64
Lys 2				H^{ϵ}_2 2.94, H^{δ}_2 1.72
Leu[h]				H^{γ} 1.70, H^{δ}_3 0.87
				H^{γ} 1.93, H^{δ}_3 0.90

[a] Solution conditions were 8 mM, pH 3.1, and 25 °C. Due to the lack of sequential NOEs, a number of spin systems could only be assigned to residue type or a class of residues. [b] AMX refers to the αH–βH_2 connectivities characteristic of the remaining two Asp and Tyr-110. Long chain refers to the remaining two Arg, two Lys, five Leu, five Glu, Ile-120, and met-124. [c] Additional AMX and Arg systems are observed. It has not been determined whether these are due to contaminants or a consequence of Pro-132 being present as both cis and trans conformers. [d] These systems were observed at 45 °C. [e] There is a sequential NOE between the NH of long chain 6 and the H^{α} of long chain 7. As there are several cases where two neighboring spin systems are long chain, specific assignments are not possible. [f] These resonances were assigned on the basis of their pH dependence (see text). [g] This system was only observed at pH 3.1 in ^2H_2O. [h] One of these systems may be the βH–γH^3 connectivity of Ile-120.

Discussion

It is rare for an isolated linear peptide fragment to possess stable ordered structure in aqueous solutions. When techniques such as circular dichroism indicate an ordered structure, we may consider this only as a measure of the average conformation of the peptide backbone fluctuating over a wide range of structures. Stability may be achieved by additional interactions with other parts of the parent protein, and consequently, as a stable structure is necessary for an NOE to occur between a proton pair, NOEs may not be observed for a peptide even when other techniques indicate an ordered conformation exists. Conversely, nonregular structures such as reverse turns and Ω-loops may not require additional tertiary interactions for stability, and therefore, peptide fragments of regions containing these structures may have sufficient stability to allow the generation of NOEs.

At this stage of our studies we have observed NOEs in the segments 96–107 and 130–133, implying that these parts of the peptide fragment are in stable structures. The majority of both segments are defined by NOEs between H^{α}_i and NH_{i+1}, indicating that these parts of the protein are extended chain. Other NOEs between backbone protons, particularly the NOE between the NH protons of Leu-101 and Val-102, and the presence of Pro-132 disturb the regularity of these extended chains. The ring protons of Tyr-110 show a number of long-range NOEs to protons distant in the primary sequence, and these NOEs, particularly those to the H^{β} of Ser-100 and Phe-103 and the H^{α} of Asp-107 (Figure 3C),

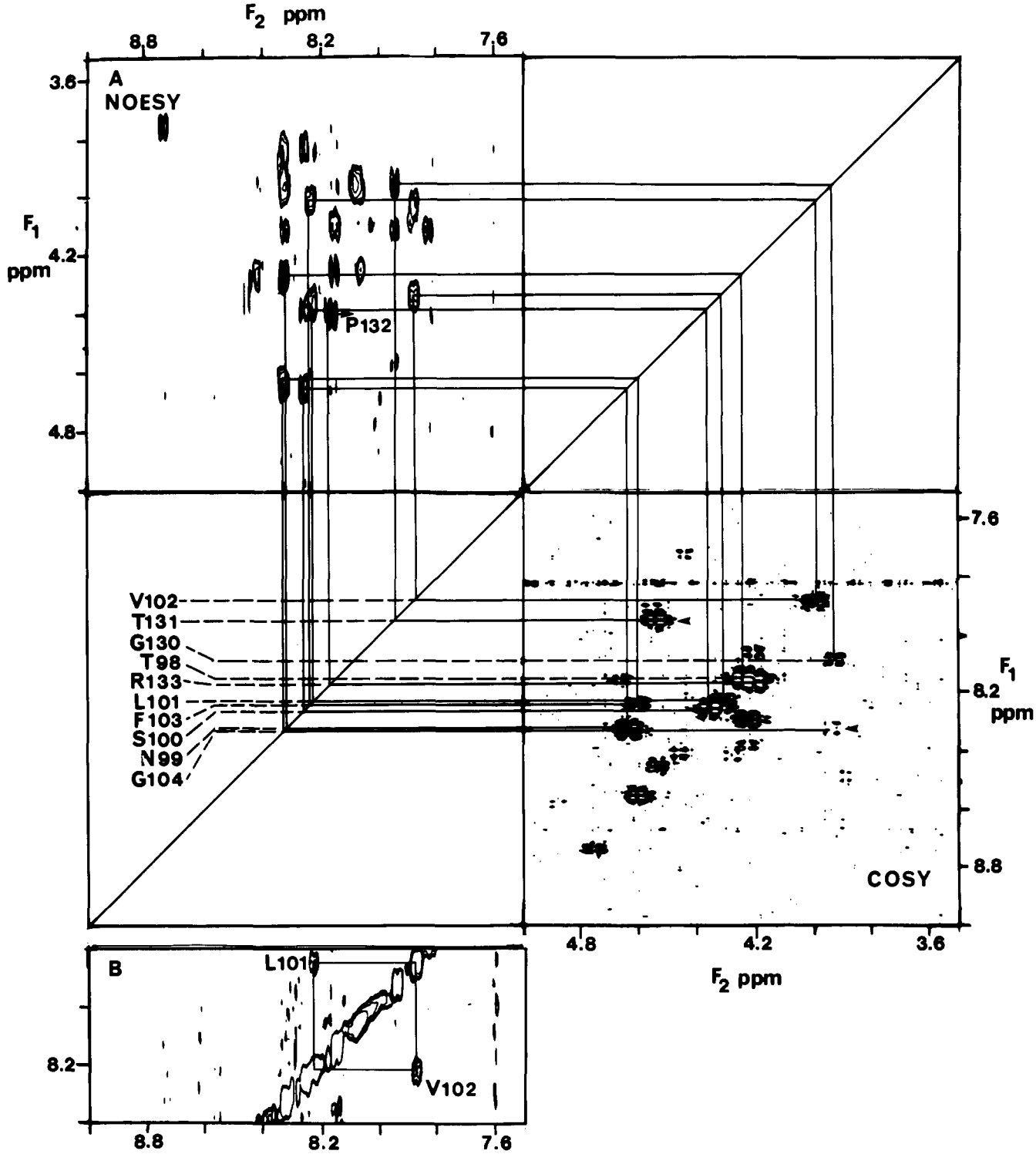

FIGURE 4: (A) Combined DQF-COSY and NOESY diagram for sequential resonance assignments via NOEs between NH_{i+1} and H^{α}_{i} of neighboring residues. In the upper left is the spectral region F_1 3.5–5.0 ppm and F_2 7.5–9.0 ppm of a NOESY spectrum of 8 mM AII in H_2O, pH 3.1 at 25 °C, recorded with a mixing time of 200 ms and 256 t_1 points. In the lower right is the spectral region F_1 7.5–9.0 ppm and F_2 3.5–5.0 ppm of a DQF-COSY acquired under the same conditions as the NOESY spectrum except with 640 t_1 points. The combination of the two spectra shows spin–spin couplings for NH_i to H^{α}_{i} and NOEs from NH_{i+1} to H^{α}_{i}. Connectivities are shown for segments 98–104, 130–131, and 132–133. The connectivities begin as the C-terminal of a segment and proceed in a clockwise direction toward the N-terminal. Starting points are indicated by horizontal arrows. (B) The spectral region F_1 7.8–8.4 ppm and F_2 7.5–9.0 ppm of the same NOESY spectrum as shown in (A). An NOE between the NH protons of Leu-101 and of Val-102 is indicated.

indicate that the peptide folds into a nonregular structure. Preliminary computations of the structure of the peptide segment 96–110 with the NOE data as distance constraints indicate an Ω-loop structure spanning residues Ser-100 to Tyr-110 (Gooley et al., unpublished results).

The absence of NOEs in the segment 110–129 where the putative helix occurs may imply that this part of the peptide is not stable. However, circular dichroism shows that helix content is concentration dependent, and modeling of the helix indicates that it is amphipathic, suggesting that the helix is stabilized through association. Consequently, the absence of NOEs indicative of a helix may be an artifact of association rather than stability. We are currently studying the effect of various solvents on helix formation and association.

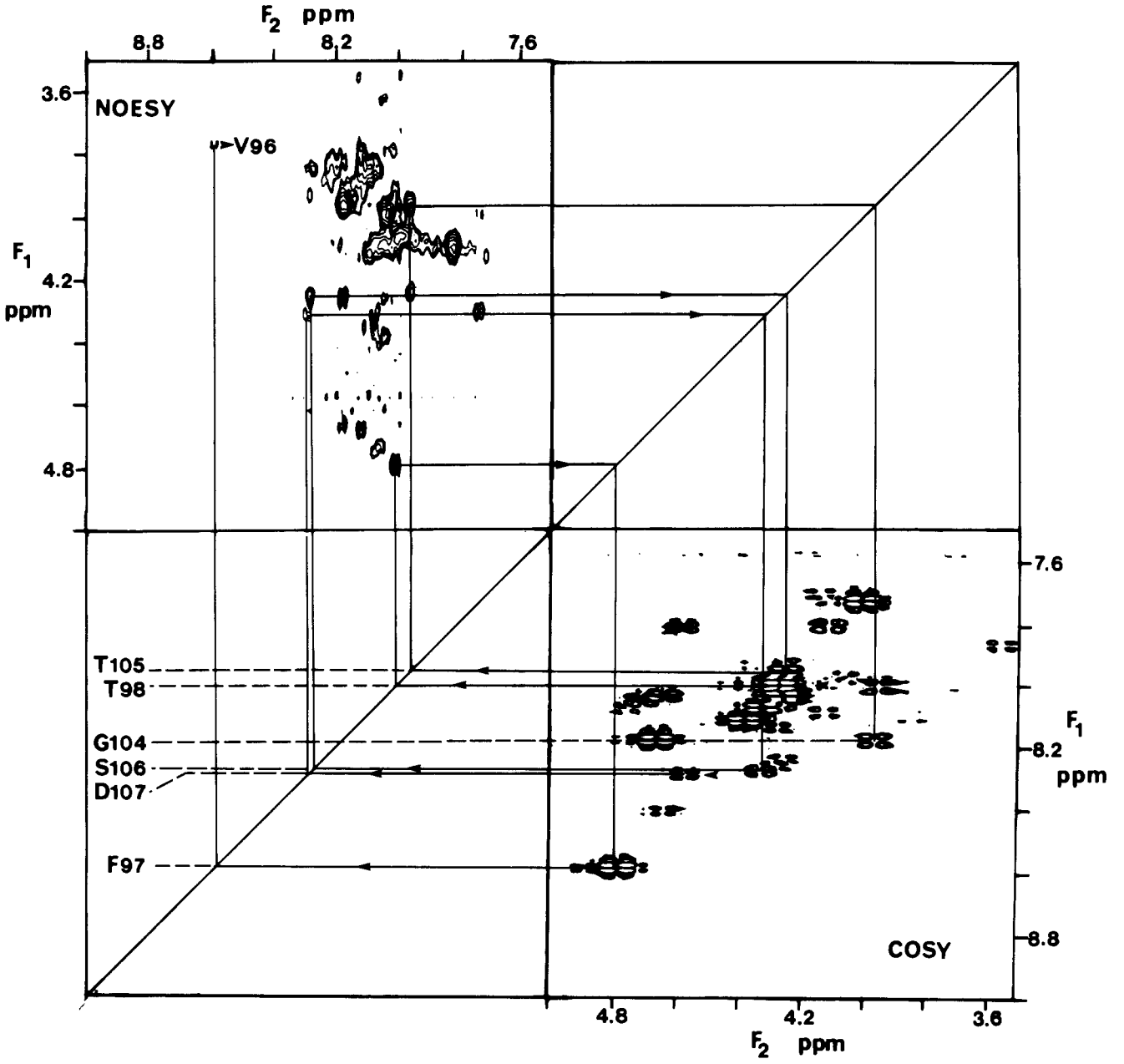

FIGURE 5: Combined DQF-COSY and NOESY diagram for sequential assignments between NH_{i+1} and H^{α}_{i} of neighboring residues. In the upper left is the spectral region F_1 3.5–5.0 ppm and F_2 7.5–9.0 ppm of a NOESY spectrum of 8 mM AII in H_2O, pH 3.1 at 45 °C, recorded with a mixing time of 200 ms and 352 t_1 points. In the lower right is the spectral region F_1 7.5–9.0 ppm and F_2 3.5–5.0 ppm of a DQF-COSY recorded under the same conditions as the NOESY spectrum. The combination of the two spectra shows spin–spin couplings for NH_i to H^{α}_{i} and NOEs from NH_{i+1} to H^{α}_{i}. Connectivities are shown for the segments 96–98 and 104–107. The connectivities begin at the C-terminal of a segment and proceed in a clockwise direction toward the N-terminal. Starting points are indicated by horizontal arrows.

In an attempt to rationalize the stability of the Ω-loop we have studied the synthetic peptide 96–112 in water (Lehrman et al., unpublished results). No NOEs were observed for this peptide, implying that this peptide has no preferred conformation. As NH exchange studies show that there are no protected amide protons in the loop region, a likely alernative is that the Ω-loop must be stabilized by internal hydrophobic interactions (Leszczynski & Rose, 1986). However, if the absence of NOEs in the segment of the helix is due to association, then the N- and C-terminal segments 96–107 and 130–133, respectively, are not associated. At 45 °C the long-range NOEs that characterize the folding of the N-terminus into an Ω-loop are weaker but apparent. Noticeably, other NOEs from the ring protons of Tyr-110 to residues containing long side chains (Figure 3B) are very weak or absent at 45 °C.

The detection of a stable Ω-loop in a protein fragment is significant for several reasons. First, a structure of this type has not previously been characterized by NMR spectroscopy. Sequential NOE data while indicative of structure do not on their own characterize ordered structure, and additional information such as NH exchange rates and chemical shifts of backbone protons is needed (Pardi et al., 1983). However, the backbone chemical shifts of residues 96–110 of AII are all nearer than 0.5 ppm of values for small peptides (Bundi & Wüthrich, 1979), and the most significant shifts are probably due to ring current effects. Further NOE data is the most useful aid for determining molecular structure (Billeter et al., 1982). For example, β-sheets are characterized by NOEs between NH_i and NH_j or H^{α}_{j}, where i and j are protons of adjacent strands, NOEs between CH_i and CH_j are especially indicative of antiparallel sheet (Wüthrich et al.,

1984; Gooley & Norton, 1986), and α-helicies can be further characterized by NOEs between NH_i andd H^{α}_{i+3} (Wüthrich et al., 1984; Clore et al., 1986). An unusual structure reported is the $\beta^{6.3}$ helix, which is characterized by both NH_i to H^{α}_{i+1} and NH_i to H^{α}_{i+6} NOEs (Arseniev et al., 1985). We have not observed any of these additional NOEs in the course of our study, and except for NOEs between side-chain protons in the neck region or internal to the Ω-loop, there are no other characteristic NOEs. However, where the neck to neck distance is less than about 6 Å (C^{α} to C^{α}; Leszczynski & Rose, 1986), NOEs between backbone protons of the neck residues may be expected.

Registry No. AII, 111524-50-6.

REFERENCES

Arseniev, A. S., Kondakov, V. I., Maiorov, V. N., & Bystrov, V. F. (1984) *FEBS Lett. 165*, 57–62.

Arseniev, A. S., Barsukov, I. L., Bystrov, V. F., Lomize, A. L., & Ovchinnikov, Yu. A. (1985) *FEBS Lett. 186*, 168–174.

Billeter, M., Braun, W., & Wüthrich, K. (1982) *J. Mol. Biol. 155*, 321–346.

Brems, D. N., Plaisted, S. M., Havel, H. A., Kauffman, E. W., Stodola, J. D., Eaton, L. C., & White, R. D. (1985) *Biochemistry 24*, 7662–7668.

Brown, J. E., & Klee, W. A. (1971) *Biochemistry 10*, 470–476.

Bundi, A., & Wüthrich, K. (1979) *Biopolymers 18*, 285–297.

Chen, C. H., & Sonenberg, M. (1977) *Biochemistry 16*, 2110–2118.

Chou, P. Y., & Fasman, G. D. (1974a) *Biochemistry 13*, 211–222.

Chou, P. Y., & Fasman, G. D. (1974b) *Biochemistry 13*, 222–245.

Clore, G. M., Martin, S. R., & Gronenborn, A. M. (1986) *J. Mol. Biol. 191*, 553–561.

Deslauriers, R., Walter, R., & Smith, I. C. P. (1972) *Biochem. Biophys. Res. Commun. 48*, 854–859.

Dyson, H. J., Cross, K. J., Houghten, R. A., Wilson, I. A., Wright, P. E., & Lerner, R. A. (1985) *Nature (London) 318*, 480–483.

Gallego, E., Herranz, J., Nieto, J. L., Rico, M., & Santoro, J. (1983) *Int. J. Pept. Protein Res. 21*, 242–253.

Gooley, P. R., & Norton, R. S. (1986) *Biochemistry 25*, 2349–2356.

Graf, L., & Li, C. H. (1974) *Biochemistry 13*, 5408–5415.

Jeener, J., Meier, B. H., Bachmann, P., & Ernst, R. R. (1979) *J. Chem. Phys. 71*, 4546–4553.

Keim, P., Vigna, R. A., Morrow, J. S., Marshall, R. C., & Gurd, F. R. N. (1973) *J. Biol. Chem. 248*, 7811–7818.

Kim, P. S., & Baldwin, R. L. (1984) *Nature (London) 307*, 329–334.

Kuwajima, K., & Baldwin, R. L. (1983) *J. Mol. Biol. 169*, 281–297.

Leszczynski, J. F., & Rose, G. D. (1986) *Science (Washington, D.C.) 234*, 849–855.

Marion, D., & Wüthrich, K. (1983) *Biochem. Biophys. Res. Commun. 113*, 967–974.

Neuhaus, D., Wagner, G., Vasák, M., Kägi, J. H. R., & Wüthrich, K. (1985) *Eur. J. Biochem. 151*, 257–273.

Pardi, A., Wagner, G., & Wüthrich, K. (1983) *Eur. J. Biochem. 137*, 445–454.

Rance, M., Sørensen, O. W., Bodenhausen, G., Wagner, G., Ernst, R. R., & Wüthrich, K. (1983) *Biochem. Biophys. Res. Commun. 117*, 479–485.

Redfield, A. G., & Kunz, S. D. (1975) *J. Magn. Reson. 19*, 250–254.

Rico, M., Nieto, J. L., Santoro, J., Bermejo, F. J., Herranz, J., & Gallego, E. (1983) *FEBS Lett. 162*, 314–319.

Shoemaker, K. R., Kim, P. S., Brems, D. N., Marqusee, S., York, E. J., Chaiken, I. M., Stewart, J. M., & Baldwin, R. L. (1985) *Proc. Natl. Acad. Sci. U.S.A. 82*, 2349–2353.

Sonenberg, M., Kitkutani, M., Free, C. A., Nadler, A. C., & Dellacha, J. M. (1968) *Ann. NY Acad. Sci. 148*, 532–558.

States, D. J., Haberkorn, R. A., & Ruben, D. J. (1982) *J. Magn. Reson. 48*, 286–292.

Swank, R. T., & Munkres, K. D. (1971) *Anal. Biochem. 39*, 462–477.

Wagner, G., Kumar, A., & Wüthrich, K. (1981) *Eur. J. Biochem. 114*, 375–384.

Wüthrich, K. (1986) *NMR of Proteins and Nucleic Acids*, Wiley, New York.

Wüthrich, K., Billeter, M., & Braun, W. (1984) *J. Mol. Biol. 180*, 715–740.

Yamasaki, N., Shimanaka, J., & Sonenberg, M. (1975) *J. Biol. Chem. 250*, 2510–2514.